Received: 1 October 2019 | Revised: 29 July 2020 | Accepted: 5 August 2020

DOI: 10.1111/ede.12352

RESEARCH

WILEY

Regulation of the limb shape during the development of the Chinese softshell turtles

Ingrid R. Cordeiro | **Reiko Yu** | **Mikiko Tanaka**

Department of Life Science and Technology, Tokyo Institute of Technology, Yokohama, Japan

Correspondence
Mikiko Tanaka, Department of Life Science and Technology, Tokyo Institute of Technology, Yokohama 226-8501, Japan.
Email: mitanaka@bio.titech.ac.jp

Funding information
Grant-in-Aid for Scientific Research (B), Grant/Award Number: 16H04828; Grant-in-Aid for Scientific Research on Innovative Areas, Grant/Award Number: 18H04818; JSPS Postdoctoral Fellowship for Foreign Researchers, Grant/Award Number: 19F19385; Takeda Science Foundation; Fujiwara Natural History Foundation

Abstract

Interdigital cell death is an important mechanism employed by amniotes to shape their limbs; inhibiting this process leads to the formation of webbed fingers, as seen in bats and ducks. The Chinese softshell turtle *Pelodiscus sinensis* (Reptilia: Testudines: Trionychidae) has a distinctive limb morphology: the anterior side of the limbs has partially webbed fingers with claw-like protrusions, while the posterior fingers are completely enclosed in webbings. Here, *P. sinensis* embryos were investigated to gain insights on the evolution of limb-shaping mechanisms in amniotes. We found cell death and cell senescence in their interdigital webbings. Spatial or temporal modulation of these processes were correlated with the appearance of indentations in the webbings, but not a complete regression of this tissue. No differences in interdigital cell proliferation were found. In subsequent stages, differential growth of the finger cartilages led to a major difference in limb shape. While no asymmetry in bone morphogenetic protein signaling was evident during interdigital cell death stages, some components of this pathway were expressed exclusively in the clawed digit tips, which also had earlier ossification. In addition, a delay and/or truncation in the chondrogenesis of the posterior digits was found in comparison with the anterior digits of *P. sinensis*, and also when compared with the previously published pattern of digit skeletogenesis of turtles without posterior webbings. In conclusion, modulation of cell death, as well as a heterochrony in digit chondrogenesis, may contribute to the formation of the unique limbs of the Chinese softshell turtles.

KEYWORDS
Chinese softshell turtle, evolution, interdigital cell death

1 | INTRODUCTION

The shape of the interdigital regions is critical for the locomotion of tetrapods, with webbed feet being commonly found in swimming and gliding animals. In amphibians, the major mechanism for eliminating interdigital membranes is regulating cell proliferation (Cameron & Fallon, 1977). In contrast, interdigital cell death is essential to remove the webbings of amniote limbs, with differential growth of digits and interdigits

being present, but insufficient, to form free fingers (Salas-Vidal, Valencia, & Covarrubias, 2001). Thus, interdigital cell death has been proposed to be a shared trait of the amniote clade (Fallon & Cameron, 1977).

Bone morphogenetic protein (BMP) signaling is key to the induction of cell death in the limbs (Gañan, Macias, Basco, Merino, & Hurle, 1998; Kaltcheva, Anderson, Harfe, & Lewandoski, 2016; Yokouchi et al., 1996; Zou & Niswander, 1996), which integrates other signals, such as the prosurvival fibroblast growth factor (FGF) signals from the apical ectodermal ridge (AER; Hernandez-Martinez et al., 2009; Lu, Minowada & Martin, 2006; Macias, Gañan, Ros, & Hurlé, 1996; Pajni-Underwood, Wilson, Elder, Mishina, & Lewandoski, 2007). Besides cell death, cell senescence is also detected in interdigital regions and may contribute to shaping this region (Muñoz-Espín et al., 2013; Storer et al., 2013).

Amniotes with webbed hands and feet inhibit cell death through distinct mechanisms. In domestic ducks, the BMP inhibitor *Grem1* is expressed in a complementary fashion to the patterns of cell death and expression of the BMP target gene *Msx2* (Gañan et al., 1998; Merino et al., 1999). In Seba's short-tailed bats (*Carollia perspicillata*), expression of *Grem1* is coupled with expansion of *Fgf8* expression in their extensive interdigital regions (Weatherbee, Behringer, Rasweiler, & Niswander, 2006). In contrast, expansion of the interdigital area itself accounts for loss of digits in horses and camels (Cooper et al., 2014). In all of these examples, it was the modulation of BMP signaling, in intensity or space, that has been suggested to create novel patterns of interdigital cell death and limb shapes in amniotes.

To understand more about the evolution of the mechanisms that shape amniote limbs, it is important to investigate several clades among this group. To our knowledge, cell death during limb development has been investigated in only a few turtle species. Degenerating cells were observed in the AER and interdigital mesoderm of the Greek tortoise (*Testudo graeca*), a Testudinid (Pieau & Raynaud, 1976). Cell death has been detected towards the distal portion of the interdigital regions of the snapping turtle (*Chelydra serpentina*), a Chelydrid, and the painted turtle (*Chrysemys picta*), an Emydid (Fallon & Cameron, 1977); both of these species have claws in all five digits, which are not joined by webbings. However, the pattern of cell death in the limbs of turtles with webbed fingers has not been investigated. In this context, Trionychids as the Chinese softshell turtle (*Pelodiscus sinensis*) are a great model due to their unique paddle-like limbs: while their anterior side is partially webbed with three protruding claws formed by the distal phalanges of the fingers i, ii, and iii, the posterior part of their hands and feet is completely webbed (Figure 1a). This wider shape makes three-clawed turtles suited for rapid turns while hunting underwater in a rowing motion, unlike the flippers of marine turtles or of pig-nosed turtles, the Trionychid's sister group (Delfino, Fritz, & Sánchez-Villagra, 2010). Here we explored how does the Chinese softshell turtle form its unique limb morphology.

2 | MATERIAL AND METHODS

2.1 | Animals

All animal experiments were performed in accordance with guidelines for animal experiments of Tokyo Institute of Technology. Eggs from the Chinese softshell turtle (*P. sinensis*) were obtained from Yamato Youshoku farm and incubated covered by humid peat moss at 30°C, as described (Hirasawa et al., 2015). Embryos were staged according to Tokita-Kuratani (TK) stages (Tokita & Kuratani, 2001).

2.2 | Detection of cell death and cell senescence in whole-mount samples

Cell death was detected in nonfixed embryos using Lysotracker green (Invitrogen; Cordeiro et al., 2019; Fogel, Thein, & Mariani, 2012). Limbs were incubated with

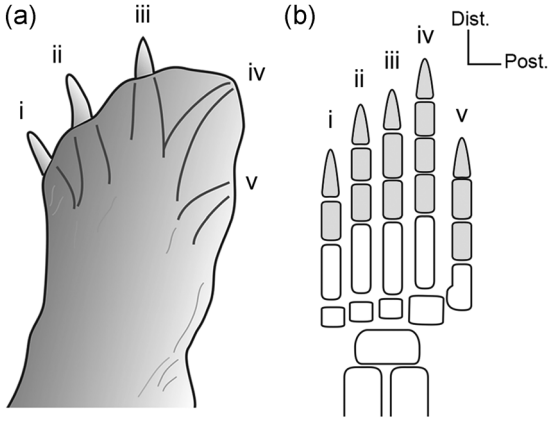

FIGURE 1 Limb morphology of the turtle *Pelodiscus sinensis*. (a) Illustration of the hindlimb of an adult Chinese softshell turtle. Its forelimbs and hindlimbs have a general paddle-like shape, with three protruding claws on its anterior side; the claws are the distal phalanges of the digits i, ii, and iii (Delfino et al., 2010). The posterior digits iv and v are completely enclosed in webbings. (b) Representation of the skeletal elements of an adult hindlimb, based on previous reports (Sánchez-Villagra et al., 2009); the phalangeal formula of the pes is 2-3-3-4-3. Phalanges are colored in gray. i–v, digits i–v; Dist., distal; post., posterior

Lysotracker green in phosphate-buffered saline (PBS) + (PBS pH 7.4, 9 mM $CaCl_2$, 3.3 mM $MgCl_2$) for 1 h at 37°C, washed with PBS + and photographed immediately. The same samples were then used for senescence staining.

The senescence-associated beta-galactosidase staining was performed as described before (Debacq-Chainiaux, Erusalimsky, Campisi, & Toussaint, 2009). Briefly, the samples were fixed in paraformaldehyde 4% overnight at 4°C, washed in PBS, incubated at 37°C in the staining solution (1 mg/ml X-gal, 40 mM citric acid/sodium phosphate buffer pH 6.0, 5 mM potassium hexacyanoferrate (II) trihydrate, 5 mM potassium hexacyano-ferrate (III), 150 mM NaCl and 2 mM $MgCl_2$) for 2–3 h, washed in PBS and observed.

Confocal images were captured using the LSM780 confocal microscope (Zeiss). Maximum intensity projections were generated using Zen Black software (Zeiss). Lysotracker-positive cells were counted using the fiji Cell Counter plugin (http://fiji.sc). The significance ($p \leq .05$) between each interdigital region was calculated using ordinary one-way analysis of variance (ANOVA) and Tukey's multiple comparisons test (GraphPad Prism v. 8.4.2).

2.3 | Probe synthesis and in situ hybridization

Total RNA was extracted from stage TK18 embryos using the RNeasy Mini Kit (Qiagen). Complementary DNA (cDNA) was synthesized by reverse transcription and used as a template for polymerase chain reaction. The *P. sinensis Grem1* gene was amplified with primers based on a Genbank-deposited sequence (XM_006132689.3; fw 5′–ATCGATAAGCTTGATGAGCAGGATGGTCC–3′ and rev 5′–CTGCAGGAATTCGATCTGCAGAATCTAG–3′) and cloned into the pBSII-SK(+) vector. Probes were transcribed using T3 (Promega) RNA polymerase and DIG RNA labeling mix (Roche). *P. sinensis Bmp2*, *Bmp4*, *Fgf8*, *Msx1*, and *Msx2* probes were prepared as before (Kuraku, Usuda, & Kuratani, 2005). In situ hybridization was performed as described for chicken embryos (Wilkinson, 1992).

2.4 | Cell-proliferation assay

Cell proliferation was detected using anti-phospho-histone H3 antibodies, as described before (Cordeiro et al., 2019; Suzuki, Satoh, Ide, & Tamura, 2007). Briefly, limbs fixed overnight with 4% paraformaldehyde were embedded in OCT compound (Tissue Tek) and sectioned at 10 μm. Sections were blocked with 1% normal goat serum/0.1% Triton X-100/0.02% Tween 20 and incubated with 1:500 rabbit anti-phospho-histone H3 (06-570, Millipore) overnight at 4°C. Secondary detection of antibodies was carried out using 1:500 goat anti-rabbit Alexa Fluor-594 conjugated antibodies (06-570, Millipore) for 2 h at room temperature. Nuclear counterstaining was performed with Hoechst 33342 solution (Invitrogen).

The cell proliferation ratio was shown as number of pH3-positive cells divided by area (mm^2) and normalized by cell density (number of nuclei in a 0.15 mm^2 rectangle). The significance of the cell proliferation ratio between each interdigital region and each stage was calculated using two-way ANOVA and Tukey's multiple comparisons test (GraphPad Prism v. 8.4.2). Significance was defined as $p \leq .05$.

2.5 | Skeleton staining

Skeletons were stained according to standard protocols using Alcian blue for cartilage and Alizarin red for bone (Ojeda, Barbosa, & Bosque, 1970).

3 | RESULTS

3.1 | Pattern of cell death and cell senescence in the limbs of the Chinese softshell turtle (*P. sinensis*)

Initially, the cell death pattern was investigated in the limbs of Chinese softshell turtles staged as previously reported (Tokita & Kuratani, 2001). Turtles were investigated in two digital plate stages (TK17 and TK19) and two later stages (TK20 and TK22) with a more mature morphology (Figure 1a). Cell death was detected in a proximal portion of the interdigital regions of both fore- and hindlimbs (forelimb $n = 5$; hindlimb $n = 5$), as well as in the AER at stage TK17 (Figure 2a,b). In the next stage, dying cells in the interdigital region were detected in a more distal position, throughout the distal-most third of the mesenchyme and also the AER (TK19, forelimb $n = 5$; hindlimb $n = 5$; Figure 2a,b). Since indentations in the interdigital webbings became more evident at this stage, the contribution of cell death was quantified in each interdigit. We found significantly more cell death in the first interdigital region (ID1) of stage TK17 forelimbs when compared to the posterior regions ID3 and ID4, while no significant differences were found at stage TK19 forelimbs (Figure S1a). Similarly, there was a slightly higher number of Lysotracker-positive cells in the anterior interdigits ID1 and ID2 of TK17 hindlimbs in relation to ID3 and ID4, although no

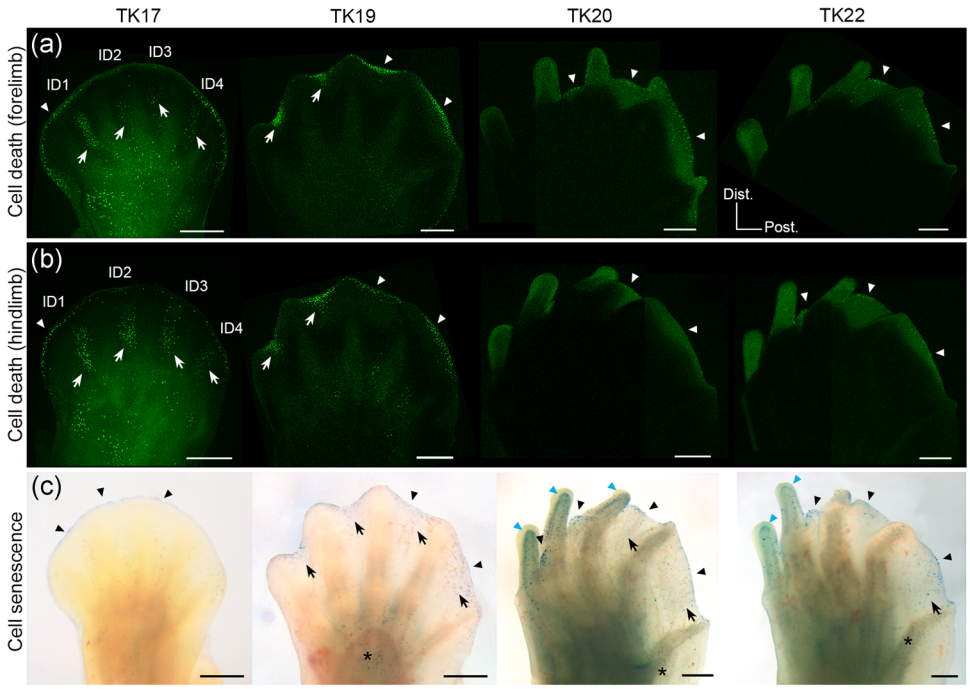

FIGURE 2 Pattern of cell death and cell senescence in the limbs of the turtle *Pelodiscus sinensis*. (a,b) Cell death (Lysotracker green staining) in forelimbs (a) and hindlimbs (b) at indicated stages. Patches of cell death in the interdigital mesenchyme (white arrows) are found proximally at stage TK17 and distally at stage TK19. In all stages, dying cells are detected in the limb margins (white arrowheads). (c) Cell senescence (senescence-associated beta-galactosidase staining) in hindlimbs. Senescent cells are present in the AER or limb margin in all investigated stages (black arrowheads). Additionally, cell senescence is found in the distal areas of cell death at stage TK19 (black arrows), but not TK17. Sparse senescent cells are found in the posterior webbings at stages TK20 and TK22 (black arrows), as well as in the tips of the digits i, ii, and iii (black arrows). Brown cells are pigment cells (asterisks), not stained cells. Panel (c, TK20) is a ventral view of the limb to evidence the staining in all interdigital regions. Panels (b, TK20 and TK22) were flipped horizontally. Panels (a,b) are maximum intensity projections of confocal image stacks including the whole interdigital region (scale bars = 500 μm). Dist., distal; ID1–4, interdigital region 1–4; post., posterior

statistical significance was detected. No differences were observed at TK19 hindlimbs (Figure S1b). Thus, cell death may play a role in shaping the webbings of the Chinese softshell turtle at digital plate stages.

At stages TK20 (forelimb $n = 3$; hindlimb $n = 3$) and TK22 (forelimb $n = 3$; hindlimb $n = 3$), cell death became restricted only to the margins of the webbings and digit tips (Figure 2a,b). The limb morphology at these later stages was more comparable to that of the adult; the claw-like digits i, ii, and iii protruded from the webbings, while digits iv and v remained almost completely webbed. Since a similar pattern of cell death was found in both forelimbs and hindlimbs, as well as in other experiments performed in this paper, results hereafter will be illustrated only by the hindlimb data.

Next, the distribution of cell senescence was investigated in the same specimens used for cell death staining. In stage TK17 limbs (forelimb $n = 2$; hindlimb $n = 3$), senescent cells were found in the AER, especially towards the anterior region (Figure 2c). Cell senescence was not detected in interdigital regions at this stage. In contrast, cell senescence was found both in the limb margins and interdigital mesenchyme at stage TK19 (forelimb $n = 4$; hindlimb $n = 4$; Figure 2c); stained senescent cells had an identical distribution to that of cell death in the anterior interdigits (ID1 and ID2), and a more widespread pattern in the posterior interdigits (ID3 and ID4), but never as proximal as found in chicken or mice limbs at equivalent stages (Lorda-Diez, Garcia-Riart, et al., 2015; Muñoz-Espín et al., 2013; Storer et al., 2013). In stages TK20 (forelimb $n = 3$; hindlimb $n = 3$) and TK22 (forelimb $n = 3$; hindlimb $n = 3$), cell senescence was found in the limb margins of limbs and throughout the webbings, as well as around the tips of the anterior digits i, ii, and iii (Figure 2c). Similarly, senescent cells have been detected in the tips of E15.5 mice nails, after interdigital membranes have regressed (Storer et al., 2013).

In conclusion, cell death and senescence in the limbs of the Chinese softshell turtle were detected in a pattern consistent with the mature limb shape of this species. Cell death was initially detected throughout all interdigital regions, with the number of dying cells being slightly more abundant in anterior regions. In older

limbs, both dying and senescent cells were restricted to the distal portion of the limbs. Thus, cell death and senescence may play a role in the regression of at least part of the webbings of *P. sinensis* limbs.

3.2 | *Fgf8* expression and cell proliferation in the interdigital regions of the Chinese softshell turtle (*P. sinensis*)

The prosurvival FGF signals secreted by the AER inhibit interdigital cell death in chicken and mice (Hernandez-Martinez et al., 2009; Macias et al., 1996; Pajni-Underwood et al., 2007). In addition, *Fgf8* is expressed in the interdigital mesenchyme of bat wings, what has been correlated with the expansion of this tissue (Weatherbee et al., 2006). Thus, this gene's expression was investigated in the Chinese softshell turtle's limbs. *Fgf8* was strongly expressed in the AER of the turtle limb buds (forelimb $n = 3$; hindlimb $n = 2$; Figure 3a), as described before (Kuraku et al., 2005). At stage TK17, expression of *Fgf8* could still be detected in the disappearing AER, from interdigits 1 to 3, but not in the interdigital mesenchyme (forelimb $n = 2$; hindlimb $n = 2$; Figure 3b). The expression pattern followed the same pattern of cell senescence (Figure 2c), as reported in the AER of mice (Storer et al., 2013). Moreover, *Fgf8* expression could not be detected neither in the AER nor in the interdigital regions at later stages (TK19, forelimb $n = 3$, hindlimb $n = 3$; and TK22, forelimb $n = 3$, hindlimb $n = 3$; Figure 3c,d).

Seeing that the regulation of cell proliferation is the main mechanism to determine the formation or absence of interdigital membranes in amphibians (Cameron & Fallon, 1977), we sought to identify if it was present in *P. sinensis*. For this, immunostaining with the mitosis marker phosphorylated histone 3 (pH3) was performed (Figure 3e). Cell proliferation ratio was calculated in relation to the interdigital area in each section, and normalized by cell density. Although cell density decreased with age, no difference was found between each interdigital region (Figure 3f). We observed that the proliferation ratio was greater at stage TK17 (hindlimb, $n = 4$), which decreased at stage TK19 (hindlimb, $n = 4$) and further at TK20 (hindlimb, $n = 4$) and TK22 (hindlimb, $n = 4$; Figure 3f). No statistical difference in the number of proliferative cells was found between each interdigital region in any of the investigated stages (Figure 3f).

In summary, neither the *Fgf8* expression pattern nor cell proliferation analysis suggest that differential growth is a critical process in regulating the different sizes of the anterior (ID1, ID2) and posterior (ID3, ID4) interdigital webbings of *P. sinensis* limbs.

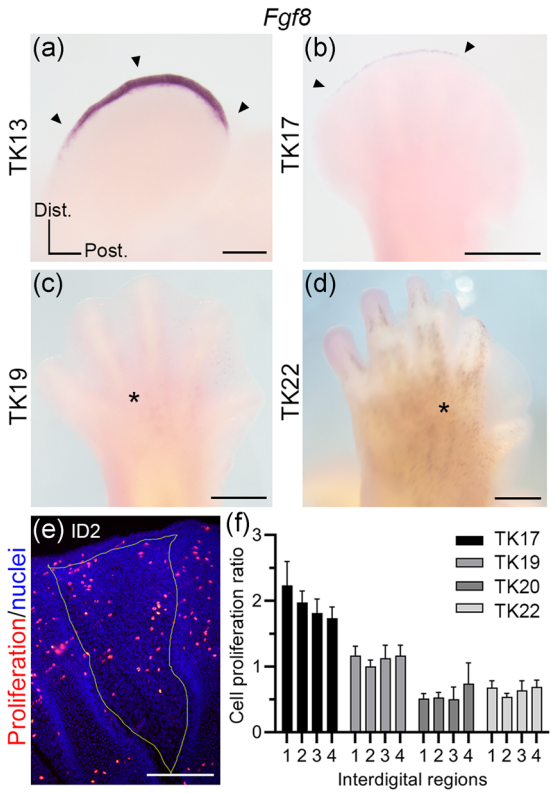

FIGURE 3 Growth of the interdigital regions of the turtle *Pelodiscus sinensis*. (a–d) Expression of *Fgf8* observed by in situ hybridization in the indicated stages. *Fgf8* is expressed in the apical ectodermal ridge (arrowheads) in a limb bud stage (a, TK13) and partially in a digit plate stage (b, TK17). No *Fgf8* expression is found at later stages (c and d, TK19 and TK22). (e) Representative image of the cell proliferation analysis (red, anti-pH3; blue, Hoechst) at stage TK19, ID2. Only cells in the interdigital regions (yellow outline) were counted. (f) Cell proliferation ratio (pH3-positive cells divided by area and cell density) according to interdigital region and stage. Two-way ANOVA with Tukey's multiple comparisons test. The source of variation was the stage ($p < .0001$), but not the interdigital region ($p = .6265$). No significant difference was found when comparing the interdigital regions within a same stage. Mean ± SEM, $n = 4$ each. Cell density varied according to stage, but not interdigital region (Stage TK17: ID1, 180 ± 15.21; ID2, 184.25 ± 21.81; ID3, 177 ± 12.31; ID4, 185.75 ± 13.15. Stage TK19: ID1, 144.5 ± 8.70; ID2, 146.75 ± 1.71; ID3, 142.5 ± 9.04; ID4, 133.5 ± 13.67. Stage TK20: ID1, 106.33 ± 20.55; ID2, 114 ± 18.13; ID3, 111 ± 27.94; ID4, 106 ± 23.96. Stage TK22: ID1, 91 ± 8.25; ID2, 87 ± 10.71; ID3, 92.75 ± 8.34; ID4, 97.25 ± 19.62. Mean ± *SD*, $n = 4$ each). Brown cells are pigment cells (asterisks), not stained cells. Panels (a–d) were flipped horizontally. Scale bars: 200 μm (a,e) and 500 μm (b–d). Dist., distal; ID2, interdigital region 2; post., posterior

3.3 | Expression of BMP-related genes during interdigital cell death stages in the Chinese softshell turtle (*P. sinensis*)

The next aim was to investigate the expression of genes associated with the regulation of interdigital cell death in

amniotes, the BMP target gene *Msx2* and the BMP inhibitor *Grem1,* through several developmental stages. Before investigating the stages in which regression of interdigital webbings was taking place, expression of these genes was validated in younger limb buds. *Msx2* was expressed in turtle limb buds (forelimb $n = 2$; hindlimb $n = 3$) as described before (Kuraku et al., 2005) (Figure 4a). *Grem1* expression (forelimb n = 3; hindlimb $n = 2$; Figure 4b) followed the typical pattern found in other amniote limbs during the outgrowth phase, when the SHH/GREM1/FGF self-regulatory system takes place (Bénazet et al., 2009; Nissim, Hasso, Fallon, & Tabin, 2006; Zúñiga, Haramis, McMahon, & Zeller, 1999). The expression of *Fgf8* and *Shh* in *P. sinensis* was also previously identified as similar to the one described in chicken and mouse (Kuraku et al., 2005).

Then, the expression pattern of these genes was investigated during interdigital cell death stages (Figures 4c–j and S2). *Msx2* was expressed in interdigital regions and distal mesenchyme of TK17 turtles (forelimb $n = 3$; hindlimb $n = 2$; Figure 4c), as also observed in chicken and mouse (Fernández-Terán, Hinchliffe, & Ros, 2006). No difference between anterior and posterior expression was detected at this stage (Figure 4c). *Msx1* also showed similar expression pattern (Figure S2a). At interdigital cell death stage, *Bmp2*, but not *Bmp4*, was expressed in the interdigital region (Figures S2b and S2c). *Msx2* expression at stage TK19 (forelimb $n = 4$; hindlimb $n = 3$) had started to disappear from the middle of the interdigital regions; interestingly, a strong expression remained in the tips of digits i, ii, and iii, but not iv or v (Figure 4e). Such expression in the digit tips was also observed at stage TK20 (forelimb $n = 2$; hindlimb $n = 2$; Figure 4g), similar to that of mouse limbs (Fernández-Terán et al., 2006; Reginelli, Wang, Sassoon, & Muneoka, 1995).

Grem1 was weakly expressed in a proximal domain in the interdigital regions at stages TK17 (forelimb $n = 3$; hindlimb $n = 3$) and TK19 (forelimb $n = 3$; hindlimb $n = 3$), showing no asymmetry between anterior and posterior regions (Figures 4d and 4f). A proximal domain of *Grem1* expression had also been reported in the interdigital regions of avians, which disappears before interdigital cell death stages in chickens, but not ducks (Merino et al., 1999). In the latter species, *Msx2* is excluded from the *Grem1*-positive domain (Gañan et al., 1998; Merino et al., 1999). Since expression of *Bmp2* is still detected at stage TK19 (forelimb $n = 3$; hindlimb $n = 3$; Figure 4i), *Grem1* expression could be necessary for the maintenance of webbings found in this turtle's paddle-like limbs (-Figure 1a). Expression of *Grem1* was not detected at the later stages TK20 (forelimb $n = 2$; hindlimb $n = 2$) and TK22 (forelimb $n = 3$; hindlimb $n = 3$; Figures 4h and 4j).

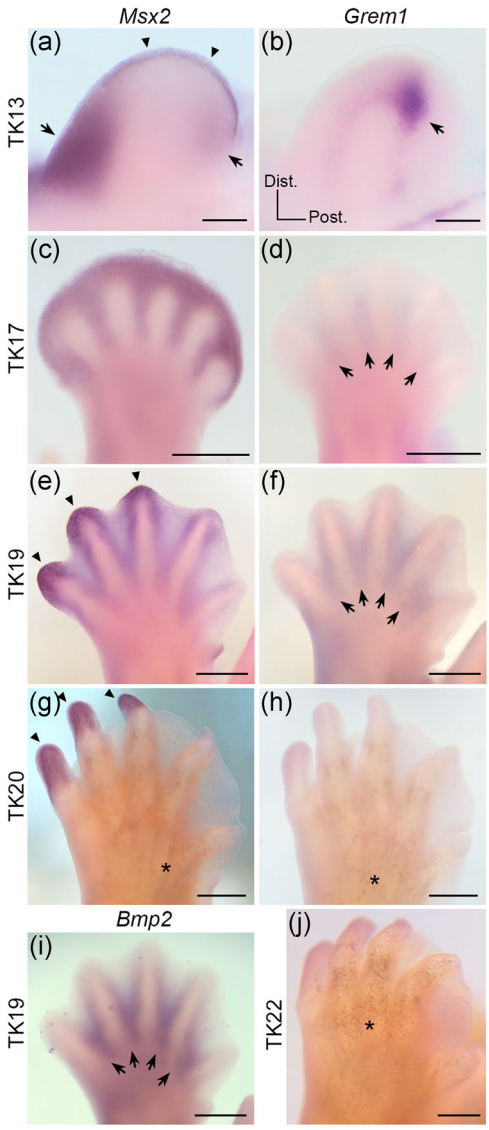

FIGURE 4 Expression of genes related to interdigital cell death in the turtle *Pelodiscus sinensis*. (a,c,e,g) Expression of the Bmp target gene *Msx2* observed by in situ hybridization. In a limb bud stage (a, TK13), *Msx2* is expressed in the apical ectodermal ridge (arrowheads) and in anterior and posterior domains (arrows). Interdigital expression is detected in the digital plate at stage TK17 (c) and have started to disappear at stage TK19 (e), when it is retained in the digit tips and stronger towards the anterior region (arrowheads). *Msx2* is expressed on the tips of the digits i, ii and iii (arrows) in a subsequent stage (g, TK20). (b,d,f,h,j) Expression of the Bmp inhibitor *Grem1* observed by in situ hybridization. *Grem1* is expressed in a conserved pattern (arrow; please see the text for details) at a limb bud stage (b, TK13). At later stages (d and f, TK17 and TK19), *Grem1* expression is detected faintly in all proximal interdigital regions (arrows), which then disappears (h, TK20; j, TK22). (i) *Bmp2* is expressed in a proximal interdigital domain at stage TK19 (arrows). Brown cells are pigment cells (asterisks), not stained cells. Panels (b,d,f,h,i) were flipped horizontally. Scale bars: 200 μm (a,b) and 500 μm (c–j). Dist., distal; post., posterior

In conclusion, the BMP target gene *Msx2* was expressed in a similar way between anterior and posterior interdigital membranes in the Chinese softshell turtle. High *Msx2* expression was found at later stages in the tips of the anterior digits, revealing that the BMP pathway may be regulating digit growth and/or differentiation. Although no clear asymmetry was observed in the expression pattern of BMP inhibitor *Grem1*, its proximal expression in addition to weaker *Msx2* expression could indicate a role in the inhibition of proximal cell death at stage TK19. Considering that the BMP ligand *Bmp2* was expressed at this stage, inhibition of cell death may be required to avoid the complete elimination of the webbings in this species.

3.4 | Bmp signaling and skeletal growth in the fingers of the Chinese softshell turtle (*P. sinensis*)

The differential expression of *Msx2* in the tips of the anterior fingers (Figures 4e and 4g) brought forward a new hypothesis regarding the formation of the uniquely shaped limbs of the Chinese softshell turtle. While BMP signaling promotes cell death in interdigital regions, these same signals also induce digit chondrogenesis and osteogenesis (Bandyopadhyay et al., 2006; Chimal-Monroy et al., 2003; Kornak & Mundlos, 2003). Thus, it is possible that differential expression of BMP ligands and/or target genes might modulate the formation of the digit skeleton in this species.

To address this question, we first investigated the finger skeletogenesis dynamics up to stage TK24, when ossification of the distal phalanges has been reported in *P. sinensis* turtles (Sánchez-Villagra et al., 2009). At stage TK19 (forelimb $n = 4$; hindlimb $n = 4$), chondrogenesis of all fingers was still in progress, as evidenced by distal digit condensations that were not completely stained by Alcian blue (Figure 5a). The claw-like terminal phalanges of the digits i, ii, and iii were first observed from the stage TK20 (forelimb $n = 4$; hindlimb $n = 4$) (Figure 5b). However, chondrogenesis of the digits iv and v had not yet been concluded by stages TK22 (forelimb $n = 6$; hindlimb $n = 6$) and TK24 (forelimb $n = 6$; hindlimb $n = 6$; Figure 5c,d). Even if ossification had already started in the terminal phalanges of the anterior digits by stage TK24 (Figure 5d)i–ii, not all phalanges had been formed by the posterior digit iv (Figure 5d) iv, as the Chinese softshell turtle pes follows the phalangeal formula of 2-3-3-4-3 (Sánchez-Villagra et al., 2009; Figure 1b). Thus, we observed a delay or truncation in the development of digits iv and v in comparison with the clawed digits i, ii, and iii.

Next, expression of the BMP ligands *Bmp2* and *Bmp4*, and the MSX transcription factors *Msx1* and *Msx2*, was investigated in a stage before the onset of ossification in distal phalanges, TK22. Interestingly, there was a difference in the expression pattern of these genes among distinct fingers. While *Bmp2* (forelimb $n = 3$; hindlimb $n = 3$) and *Msx2* (forelimb $n = 3$; hindlimb $n = 3$) were expressed only in the tips of digits i, ii, and iii (Figures 5e and 5h), *Bmp4* (forelimb $n = 3$; hindlimb $n = 3$) and *Msx1* (forelimb $n = 3$; hindlimb $n = 3$) were expressed in the tips of all digits (Figures 5f and 5g). These data suggest that differential expression of BMP signals and MSX transcription factors could be modulating the rate of chondrogenesis and/or ossification of this species' digits.

At the later stage TK24, when ossification had already started, weak *Msx1* expression was found only in the tips of digits i, ii, and iii, as seen in a ventral view (forelimb $n = 3$; hindlimb $n = 3$; Figure 5i). In two of the three investigated specimens, *Msx2* was expressed by the tips of digits i, ii, and iii as well (forelimb $n = 3$; hindlimb $n = 3$; Figure 5j). The discrepancy between the *Msx1*/*Msx2* patterns at TK22 and TK24 stages may indicate the expression timing of these digit tip markers is distinct between the anterior, clawed phalanges and the posterior, potentially truncated digit tips. This differential expression was correlated with the pattern of ossification of the fingers, as only the anterior fingers had started their ossification by TK24 (Figure 5d).

Taken together, these results suggest that multiple mechanisms are regulating the unique limb shape of three-clawed turtles, using the Chinese softshell turtle (*Pelodiscus sinensis*) as a model. At an earlier stage, interdigital cell death appears to play a minor role in reducing the partial webbings in the anterior side of their limbs. At later stages, an asymmetry of Bmp signaling was detected in the tips of the digits, which could regulate both digit extension and ossification of the phalanges. The additional expression of a BMP ligand and an MSX transcription factor at the fingers i, ii, and iii was correlated with faster maturation of the digit skeleton.

4 | DISCUSSION

Here, we investigated the development of the distinctively shaped limbs of Chinese softshell turtles (*Pelodiscus sinensis*), which can give insights about the evolution of the limb shape in amniotes. We found out that cell death and cell senescence are present in this species' interdigital webbings, as have been proposed as a common trait of amniotes. Expression of the BMP inhibitor *Grem1* and a decrease in the BMP target gene *Msx2* expression could be mediating the inhibition of

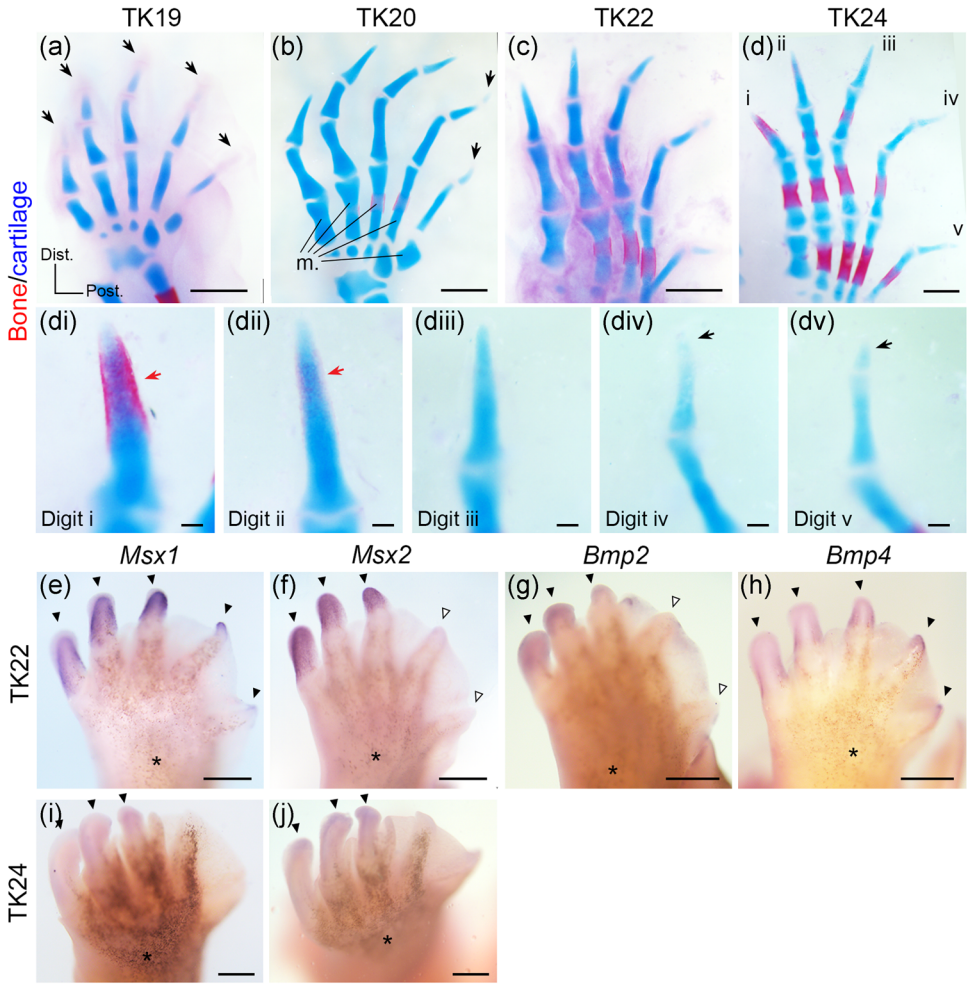

FIGURE 5 Skeletal growth and BMP signaling during digit development in the turtle *Pelodiscus sinensis*. (a–d) Bone (Alizarin red) and cartilage (Alcian blue) staining of the skeleton at the indicated stages. At stage TK19 (a), chondrogenesis is still actively taking place at the distal region of all digits (black arrows). Even if the formation of the phalangeal elements of the claw-like digits i, ii, and iii is completed from stage TK20 (b), chondrogenesis is still occurring in the digits iv and v at stage TK24 (d). A magnified view of the distal phalanges at stage TK24 is seen in panels below. The terminal phalanges are present at digits i, ii, and iii, with a bone collar (red arrows) evident in digits i and ii (d-i and d-ii). Condensations with no Alcian blue retention can still be found (black arrows) in the posterior digits iv and v, which are fully contained within the interdigital webbings (d-iv and d-v). (e–j) In situ hybridization of several BMP pathway-associated genes. At stage TK22, *Msx1* (e) and *Bmp4* (h) are expressed in the tips of all digits (black arrowheads), while *Msx2* (f) and *Bmp2* (g) are expressed only in the tips of the digits i, ii, and iii (black arrowheads), but not digits iv or v (open arrowheads). At stage TK24, both *Msx1* (i) and *Msx2* (j) are expressed only in the tips of digits i, ii, and iii. Panels (a,e,g,i) were flipped horizontally. Scale bars: 100 μm (i–v) and 500 μm (a–j). Dist., distal; m., metatarsals; post., posterior

proximal cell death and senescence, which is consistent with the general paddle-like shape of *P. sinensis* limbs. We found no evidence that differential cell proliferation or *Fgf8* expression created an asymmetry between anterior and posterior webbings. In contrast, a clear distinction in the expression of a subset of the BMP ligands and MSX transcription factors was detected in the digit tips in subsequent stages. Such expression was correlated with the formation of the clawed terminal phalanges and faster ossification of the anterior digits. Finally, a delay in chondrogenesis of the posterior, fully webbed digits was found when compared with anterior digits.

Interdigital cell death has been detected towards the distal portion of the snapping turtle's (*Chelydra serpentina*) and the painted turtle's (*Chrysemys picta*) limbs (Fallon & Cameron, 1977), both of which forms five claws with short webbings (Cordero & Janzen, 2014; Yntema, 1968). In contrast, *P. sinensis* has paddle-like limbs with partial webbings in the anterior side and complete webbings in the posterior side. Thus, it is possible that developmental mechanisms for tissue removal are present in the anterior side of their limbs, although their contribution will be understandably smaller than in species with completely individualized fingers.

Proximal domains of interdigital cell death found here have not been previously described in turtles, and were correlated with the appearance of indentations in the interdigits (Figure 2a,b). Unlike seen in chicken limbs (Lorda-Diez, Garcia-Riart, et al., 2015), interdigital cell senescence in *P. sinensis* did not appear proximally alongside cell death, being found only in a more distal position at later stages (Figure 2e), when cell death was also restricted to a distal domain (Figure 2a,b).

BMP signaling was required for regression of the interdigital membranes in many previously investigated amniote species. *Msx2* expression has been linked to variation in the interdigital cell death pattern in avian limbs (Gañan et al., 1998). Such correlation is not evident in mice, revealing that multiple mechanisms regulate the regression of the interdigital webbings in amniotes (Fernández-Terán et al., 2006). *Msx2* was also expressed for a longer time around the tips of the anterior digits of *P. sinensis*, which could affect endochondral ossification (Satokata et al., 2000) and also induce cell senescence, as this gene has been associated with developmental senescence in the chicken AER (Storer et al., 2013). The BMP inhibitor *Grem1* was not expressed in a differential way between anterior and posterior regions in the limbs of *P. sinensis*, but, as has been proposed in ducks (Merino et al., 1999) or bats (Weatherbee et al., 2006), it could mediate inhibition of proximal cell death at stage TK19 (Figure 4f) alongside a decrease in *Msx2* expression (Figure 4e). However, unlike reported in bat wings (Weatherbee et al., 2006), *Fgf8* expression was not found in the interdigital mesenchyme of *P. sinensis*, Nevertheless, FGF signals might play a role in this process through a long-term positive effect on cell death in synergy with BMP signals, as described in chicken limbs (Montero et al., 2001). Although both cell death and cell senescence were detected in *P. sinensis*, it is not possible to exclude the effect of differential growth of the fingers, which contributes to digit individualization in mice (Salas-Vidal et al., 2001). The role of Bmp signaling on both digit chondrogenesis and interdigital cell death at this stage supports a combined effect of both processes to shape limbs at the digital plate stages. Investigation of the pattern of cell death and expression of related genes in additional turtle species will reveal more about the molecular basis for the induction—or repression—of interdigital cell death in this clade.

Interestingly, an additional mechanism for shaping the limbs was present in *P. sinensis*: a delay in chondrogenesis of the posterior digits iv and v in relation to the anterior, clawed digits. Such a delay in the formation of the posterior digits has been observed in another Trionychidae turtle, *Apalone spinifera* (Sheil, 2003), but not during skeletogenesis of turtles with five claws, such as the Chelydridae turtles *Chelydra serpentina* (Sheil & Greenbaum, 2005) and *Macrochelys temminckii* (Sheil, 2005) or the Emydidae turtle *Trachemys scripta* (Sheil & Portik, 2008). It is fascinating to speculate whether the delay in the chondrogenesis of digits iv and v ensures that claw-like phalanges do not emerge from the posterior, webbed portion of the limbs of the three-clawed turtles. Ossification of the terminal phalanges of digits iv and v is not yet completed by the hatchling stage in *P. sinensis* (Sánchez-Villagra et al., 2009); this situation mirrors the one found in digits 2 and 4 of chicken wings, in which the onset of osteogenesis is nearing or after hatching, respectively (Holder, 1978). Notably, the posterior chicken wing digits are truncated, with no expression of digit tip markers or presence of terminal claws (Casanova, Badia-Careaga, Uribe, & Sanz-Ezquerro, 2012). The terminal phalanges have specific expression of several genes, including ligands of the BMP and WNT pathways, and MSX or DLX transcription factors (Casanova & Sanz-Ezquerro, 2007). Notably, *Msx1* was expressed in all digit tips of the Chinese softshell turtle, while *Msx2* was expressed only in the claw-like tips of digits i, ii, and iii (Figures 4 and 5). Developmental knockout of *Msx1*/*Msx2* in the limb mesenchyme led to the absence of terminal phalanges in mice (Bensoussan-Trigano, Lallemand, Saint Cloment, & Robert, 2011); these two genes remain expressed in the nail bed, being necessary for the regenerative response after amputation of the terminal phalanges of neonate mice (Reginelli et al., 1995). MSX1, but not MSX2, was necessary for a complete regeneration via modulation of BMP4, but not BMP2 (Han, Yang, Farrington, & Muneoka, 2003; Reginelli et al., 1995); in *P. sinensis*, *Bmp4* was also expressed in the same pattern as *Msx1*, while *Bmp2* was restricted to the anterior digits (Figure 5). Notably, cell senescence was restricted to the tips of the anterior digits (Figure 2e); senescent cells are also detected around the terminal phalanges in mice after interdigital cell death stages (Storer et al., 2013). These data suggest that regulation of BMP ligands and MSX factors could mediate the truncation of the posterior digits of the Chinese softshell turtle, which do not have terminal claws.

BMP signaling not only regulates the formation of the digit tips. After the establishment of the digit-interdigit pattern (Raspopovic, Marcon, Russo, & Sharpe, 2014), which is evident from stage TK15/16 in *P. sinensis* (Tokita & Kuratani, 2001), BMP signals regulate digit extension and identity (Huang et al., 2016; Montero, Lorda-Diez, Gañan, Macias, & Hurle, 2008; Suzuki, Hasso, & Fallon, 2008). More specifically, regulation of the activity of the phalanx-forming regions by the BMP/SMAD pathway promotes the formation of phalanges and joints, as modulated by several other limb patterning

signals including IHH, WNT, FGF, HOX, GLI3 and TGFβ (Huang et al., 2016; Sanz-Ezquerro & Tickle, 2003; Witte, Chan, Economides, Mundlos, & Stricker, 2010). This points to a mechanism that is able to slow down the process of digit chondrogenesis in *P. sinensis* limbs, but without exhausting the pool of prechondrogenic progenitors, which instead would lead to shorter digits (Montero et al., 2001; Sanz-Ezquerro & Tickle, 2003; Witte et al., 2010). Investigating pathways that could modulate the function of phalanx-forming regions in this species will be important to understand the delay in the chondrogenesis of their posterior digits, as well as further innovations found in Trionychids, such as hyperphalangy (Delfino et al., 2010). Thus, differential modulation of genes expressed during digit development and regeneration in amniotes is observed in the Chinese softshell turtle, revealing putative mechanisms for the evolution of novel limb shapes.

ACKNOWLEDGEMENTS

We thank Dr. Shigeru Kuratani for donating the *Bmp2*, *Bmp4*, *Fgf8*, *Msx1* and *Msx2* plasmids for RNA probes; Dr. Tatsuya Hirasawa and Dr. Bau-Lin Huang for technical advice; and the Biotechnology Center of Tokyo Institute of Technology for sequencing services. This study was supported by a JSPS Postdoctoral Fellowship for Foreign Researchers to I. R. C. (19F19385), a Grant-in-Aid for Scientific Research (B) (16H04828), a Grant-in-Aid for Scientific Research on Innovative Areas (18H04818), the Takeda Science Foundation, and the Fujiwara Natural History Foundation to M. T.

CONFLICT OF INTERESTS

The authors declare that there are no conflict of interests.

DATA AVAILABILITY STATEMENT

The data that support the findings of this study are available from the corresponding author upon reasonable request.

ORCID

Mikiko Tanaka http://orcid.org/0000-0001-8092-8594

REFERENCES

Bandyopadhyay, A., Tsuji, K., Cox, K., Harfe, B. D., Rosen, V., & Tabin, C. J. (2006). Genetic analysis of the roles of BMP2, BMP4, and BMP7 in limb patterning and skeletogenesis. *PLOS Genetics*, *2*(12), 2116–2130. https://doi.org/10.1371/journal.pgen.0020216

Bénazet, J. D., Bischofberger, M., Tiecke, E., Gonçalves, A., Martin, J. F., Zuniga, A., & Zeller, R. (2009). A self-regulatory system of interlinked signaling feedback loops controls mouse limb patterning. *Science*, *323*(5917), 1050–1053. https://doi.org/10.1126/science.1168755

Bensoussan-Trigano, V., Lallemand, Y., Saint Cloment, C., & Robert, B. (2011). Msx1 and Msx2 in limb mesenchyme modulate digit number and identity. *Developmental Dynamics*, *240*(5), 1190–1202. https://doi.org/10.1002/dvdy.22619

Cameron, J. A., & Fallon, J. F. (1977). The absence of cell death during development of free digits in amphibians. *Developmental Biology*, *55*(2), 331–338. https://doi.org/10.1016/0012-1606(77)90176-2

Casanova, J. C., Badia-Careaga, C., Uribe, V., & Sanz-Ezquerro, J. J. (2012). Bambi and Sp8 expression mark digit tips and their absence shows that chick wing digits 2 and 3 are truncated. *PLOS One*, *7*(12), 1–11. https://doi.org/10.1371/journal.pone.0052781

Casanova, J. C., & Sanz-Ezquerro, J. J. (2007). Digit morphogenesis: Is the tip different? *Development Growth and Differentiation*, *49*(6), 479–491. https://doi.org/10.1111/j.1440-169X.2007.00951.x

Chimal-Monroy, J., Rodriguez-Leon, J., Montero, J. A., Gañan, Y., Macias, D., Merino, R., & Hurle, J. M. (2003). Analysis of the molecular cascade responsible for mesodermal limb chondrogenesis: Sox genes and BMP signaling. *Developmental Biology*, *257*(2), 292–301. https://doi.org/10.1016/S0012-1606(03)00066-6

Cooper, K. L., Sears, K. E., Uygur, A., Maier, J., Baczkowski, K.-S., Brosnahan, M., & Tabin, C. J. (2014). Patterning and post-patterning modes of evolutionary digit loss in mammals. *Nature*, *511*(7507), 41–45. https://doi.org/10.1038/nature13496

Cordeiro, I. R., Kabashima, K., Ochi, H., Munakata, K., Nishimori, C., Laslo, M., Hanken, J., & Tanaka, M. (2019). Environmental oxygen exposure allows for the evolution of interdigital cell death in limb patterning. *Developmental Cell*, *50*(2), 155–166. https://doi.org/10.1016/j.devcel.2019.05.025

Cordero, G. A., & Janzen, F. J. (2014). An enhanced developmental staging table for the painted turtle, Chrysemys picta (Testudines: Emydidae). *Journal of Morphology*, *275*(4), 442–455. https://doi.org/10.1002/jmor.20226

Debacq-Chainiaux, F., Erusalimsky, J. D., Campisi, J., & Toussaint, O. (2009). Protocols to detect senescence-associated beta-galactosidase (SA-βgal) activity, a biomarker of senescent cells in culture and in vivo. *Nature Protocols*, *4*(12), 1798–1806. https://doi.org/10.1038/nprot.2009.191

Delfino, M., Fritz, U., & Sánchez-Villagra, M. R. (2010). Evolutionary and developmental aspects of phalangeal formula variation in pig-nose and soft-shelled turtles (Carettochelyidae and Trionychidae). *Organisms Diversity and Evolution*, *10*(1), 69–79. https://doi.org/10.1007/s13127-010-0019-x

Fallon, J. F., & Cameron, J. (1977). Interdigital cell death during limb development of the turtle and lizard with an interpretation of evolutionary significance. *Journal of Embryology and Experimental Morphology*, *40*, 285–289.

Fernández-Terán, M. A., Hinchliffe, J. R., & Ros, M. A. (2006). Birth and death of cells in limb development: A mapping study. *Developmental Dynamics*, *235*(9), 2521–2537. https://doi.org/10.1002/dvdy.20916

Fogel, J. L., Thein, T. Z. T., & Mariani, F. V. (2012). Use of lysotracker to detect programmed cell death in embryos and differentiating embryonic stem cells. *Journal of Visualized Experiments*, *68*, e4254. https://doi.org/10.3791/4254

Gañan, Y., Macias, D., Basco, R. D., Merino, R., & Hurle, J. M. (1998). Morphological diversity of the avian foot is related with the pattern of msx gene expression in the developing autopod. *Developmental Biology*, *196*(1), 33–41. https://doi.org/10.1006/dbio.1997.8843

Han, M., Yang, X., Farrington, J. E., & Muneoka, K. (2003). Digit regeneration is regulated by Msx1 and BMP4 in fetal mice. *Development*, *130*(21), 5123–5132. https://doi.org/10.1242/dev.00710

Hernandez-Martinez, R., Castro-Obregon, S., Covarrubias, L., Hernández-martínez, R., Castro-obregón, S., & Covarrubias, L. (2009). Progressive interdigital cell death: Regulation by the antagonistic interaction between fibroblast growth factor 8 and retinoic acid. *Development*, *136*(21), 3669–3678. https://doi.org/10.1242/dev.041954

Hirasawa, T., Pascual-Anaya, J., Kamezaki, N., Taniguchi, M., Mine, K., & Kuratani, S. (2015). The evolutionary origin of the turtle shell and its dependence on the axial arrest of the embryonic rib cage. *Journal of Experimental Zoology Part B: Molecular and Developmental Evolution*, *324*(3), 194–207. https://doi.org/10.1002/jez.b.22579

Holder, N. (1978). The onset of osteogenesis in the developing chick limb. *Journal of Embryology and Experimental Morphology*, *44*, 15–29. https://dev.biologists.org/content/44/1/15

Huang, B. L., Trofka, A., Furusawa, A., Norrie, J. L., Rabinowitz, A. H., Vokes, S. A., & Mackem, S. (2016). An interdigit signalling centre instructs coordinate phalanx-joint formation governed by 5′Hoxd–Gli3 antagonism. *Nature Communications*, *7*, 12903. https://doi.org/10.1038/ncomms12903

Kaltcheva, M. M., Anderson, M. J., Harfe, B. D., & Lewandoski, M. (2016). BMPs are direct triggers of interdigital programmed cell death. *Developmental Biology*, *411*(2), 266–276. https://doi.org/10.1016/j.ydbio.2015.12.016

Kornak, U., & Mundlos, S. (2003). Genetic disorders of the skeleton: A developmental approach. *American Journal of Human Genetics*, *73*(3), 447–474. https://doi.org/10.1086/377110

Kuraku, S., Usuda, R., & Kuratani, S. (2005). Comprehensive survey of carapacial ridge-specific genes in turtle implies co-option of some regulatory genes in carapace evolution. *Evolution & Development*, *17*, 3–17. https://doi.org/10.1111/j.1525-142X.2005.05002.x

Lorda-Diez, C. I., Garcia-Riart, B., Montero, J. A., Rodriguez-León, J., Garcia-Porrero, J. A., & Hurlé, J. M. (2015). Apoptosis during embryonic tissue remodeling is accompanied by cell senescence. *Aging*, *7*(11), 974–985. https://doi.org/10.18632/aging.100844

Lu, P., Minowada, G., & Martin, G. R. (2006). Increasing Fgf4 expression in the mouse limb bud causes polysyndactyly and rescues the skeletal defects that result from loss of Fgf8 function. *Development*, *133*(1), 33–42. https://doi.org/10.1242/dev.02172

Macias, D., Gañan, Y., Ros, M. A., & Hurlé, J. M. (1996). In vivo inhibition of programmed cell death by local administration of FGF-2 and FGF-4 in the interdigital areas of the embryonic chick leg bud. *Anatomy and Embryology*, *193*(6), 533–541. https://doi.org/10.1007/BF00187925

Merino, R., Rodriguez-Leon, J., Macias, D., Gañan, Y., Economides, A. N., & Hurle, J. M. (1999). The BMP antagonist Gremlin regulates outgrowth, chondrogenesis and programmed cell death in the developing limb. *Development*, *126*(23), 5515–5522. https://dev.biologists.org/content/126/23/5515

Montero, J. A., Gañan, Y., Macias, D., Rodriguez-Leon, J., Sanz-Ezquerro, J. J., Merino, R., & Hurle, J. M. (2001). Role of FGFs in the control of programmed cell death during limb development. *Development*, *128*(11), 2075–2084. https://dev.biologists.org/content/128/11/2075

Montero, J. A., Lorda-Diez, C. I., Gañan, Y., Macias, D., & Hurle, J. M. (2008). Activin/TGFβ and BMP crosstalk determines digit chondrogenesis. *Developmental Biology*, *321*(2), 343–356. https://doi.org/10.1016/j.ydbio.2008.06.022

Muñoz-Espín, D., Cañamero, M., Maraver, A., Gómez-López, G., Contreras, J., Murillo-Cuesta, S., & Serrano, M. (2013). Programmed cell senescence during mammalian embryonic development. *Cell*, *155*(5), 1104–1118. https://doi.org/10.1016/j.cell.2013.10.019

Nissim, S., Hasso, S. M., Fallon, J. F., & Tabin, C. J. (2006). Regulation of Gremlin expression in the posterior limb bud. *Developmental Biology*, *299*(1), 12–21. https://doi.org/10.1016/j.ydbio.2006.05.026

Ojeda, J. L., Barbosa, E., & Bosque, P. G. (1970). Selective skeletal staining in whole chicken embryos; a rapid alcian blue technique. *Stain Technology*, *45*(3), 137–138. https://doi.org/10.3109/10520297009085357

Pajni-Underwood, S., Wilson, C. P., Elder, C., Mishina, Y., & Lewandoski, M. (2007). BMP signals control limb bud interdigital programmed cell death by regulating FGF signaling. *Development*, *134*, 2359–2368. https://doi.org/10.1242/dev.001677

Pieau, C., & Raynaud, A. (1976). Cellular degeneration in the apical crest of the limb bud of the moorish turtle (Testudo graeca L., Chelonian) (*Comptes Rendus Hebdomadaires Des Séances de l'Académie Des Sciences*). *Série D, Sciences Naturelles*, *282*, 1797–1800. https://gallica.bnf.fr/ark:/12148/bpt6k54844424/f253.item

Raspopovic, J., Marcon, L., Russo, L., & Sharpe, J. (2014). Digit patterning is controlled by a Bmp-Sox9-Wnt Turing network modulated by morphogen gradients. *Science*, *345*(6196), 566–570. https://doi.org/10.1126/science.1252960

Reginelli, A. D., Wang, Y. Q., Sassoon, D., & Muneoka, K. (1995). Digit tip regeneration correlates with regions of Msx1 (Hox 7) expression in fetal and newborn mice. *Development*, *121*(4), 1065–1076. https://dev.biologists.org/content/121/4/1065

Salas-Vidal, E., Valencia, C., & Covarrubias, L. (2001). Differential tissue growth and patterns of cell death in mouse limb autopod morphogenesis. *Developmental Dynamics: An Official Publication of the American Association of Anatomists*, *220*(4), 295–306. https://doi.org/10.1002/dvdy.1108

Sánchez-Villagra, M. R., Müller, H., Sheil, C. A., Scheyer, T. M., Nagashima, H., & Kuratani, S. (2009). Skeletal development in the chinese soft-shelled turtle *Pelodiscus sinensis* (Testudines: Trionychidae). *Journal of Morphology*, *270*, 1381–1399. https://doi.org/10.1002/jmor.10766

Sanz-Ezquerro, J. J., & Tickle, C. (2003). FGF signaling controls the number of phalanges and tip formation in developing digits.

Current Biology, *13*, 1830–1836. https://doi.org/10.1016/j.cub.2003.09.040

Satokata, I., Ma, L., Ohshima, H., Bei, M., Woo, I., Nishizawa, K., & Maas, R. (2000). Msx2 deficiency in mice causes pleiotropic defects in bone growth and ectodermal organ formation. *Nature Genetics*, *24*(4), 391–395. https://doi.org/10.1038/74231

Sheil, C. A. (2003). Osteology and skeletal development of *Apalone spinifera* (Reptilia: Testudines: Trionychidae). *Journal of Morphology*, *256*(1), 42–78. https://doi.org/10.1002/jmor.10074

Sheil, C. A. (2005). Skeletal development of *Macrochelys temminckii* (Reptilia: Testudines: Chelydridae). *Journal of Morphology*, *263*(1), 71–106. https://doi.org/10.1002/jmor.10290

Sheil, C. A., & Greenbaum, E. (2005). Reconsideration of skeletal development of Chelydra serpentina (Reptilia: Testudinata: Chelydridae): Evidence for intraspecific variation. *Journal of Zoology*, *265*(3), 235–267. https://doi.org/10.1017/S0952836904006296

Sheil, C. A., & Portik, D. (2008). Formation and ossification of limb elements in trachemys scripta and a discussion of autopodial elements in turtles. *Zoological Science*, *25*(6), 622–641. https://doi.org/10.2108/zsj.25.622

Storer, M., Mas, A., Robert-Moreno, A., Pecoraro, M., Ortells, M. C., Di Giacomo, V., & Keyes, W. M. (2013). Senescence is a developmental mechanism that contributes to embryonic growth and patterning. *Cell*, *155*(5), 1119–1130. https://doi.org/10.1016/j.cell.2013.10.041

Suzuki, M., Satoh, A., Ide, H., & Tamura, K. (2007). Transgenic Xenopus with prx1 limb enhancer reveals crucial contribution of MEK/ERK and PI3K/AKT pathways in blastema formation during limb regeneration. *Developmental Biology*, *304*(2), 675–686. https://doi.org/10.1016/j.ydbio.2007.01.019

Suzuki, T., Hasso, S. M., & Fallon, J. F. (2008). Unique SMAD1/5/8 activity at the phalanx-forming region determines digit identity. *Proceedings of the National Academy of Sciences of the United States of America*, *105*(11), 4185–4190. https://doi.org/10.1073/pnas.0707899105

Tokita, M., & Kuratani, S. (2001). Normal embryonic stages of the Chinese softshelled turtle *Pelodiscus sinensis* (Trionychidae). *Zoological Science*, *715*, 705–715. https://doi.org/10.2108/zsj.18.705

Weatherbee, S. D., Behringer, R. R., Rasweiler, J. J., & Niswander, L. A. (2006). Interdigital webbing retention in bat wings illustrates genetic changes underlying amniote limb diversification. *Proceedings of the National Academy of Sciences of the United States of America*, *103*(41), 15103–15107. https://doi.org/10.1073/pnas.0604934103

Wilkinson, D. G. (1992). In situ hybridization: a practical approach. IRL Press at Oxford University Press.

Witte, F., Chan, D., Economides, A. N., Mundlos, S., & Stricker, S. (2010). Receptor tyrosine kinase-like orphan receptor 2 (ROR2) and Indian hedgehog regulate digit outgrowth mediated by the phalanx-forming region. *Proceedings of the National Academy of Sciences of the United States of America*, *107*(32), 14211–14216. https://doi.org/10.1073/pnas.1009314107

Yntema, C. L. (1968). A series of stages in the embryonic development of Chelydra serpentina. *Journal of Morphology*, *125*(2), 219–251. https://doi.org/10.1002/jmor.1051250207

Yokouchi, Y., Sakiyama, J., Kameda, T., Iba, H., Suzuki, A., Ueno, N., & Kuroiwa, a (1996). BMP-2/-4 mediate programmed cell death in chicken limb buds. *Development*, *122*(12), 3725–3734. https://dev.biologists.org/content/134/12/2359

Zou, H., & Niswander, L. (1996). Requirement for BMP signaling in interdigital apoptosis and scale formation. *Science*, *272*(5262), 738–741. https://doi.org/10.1126/science.272.5262.738

Zúñiga, A., Haramis, A.-P. G., McMahon, A. P., & Zeller, R. (1999). Signal relay by BMP antagonism controls the SHH/FGF4 feedback loop in vertebrate limb buds. *Nature*, *401*(6753), 598–602. https://doi.org/10.1038/44157

SUPPORTING INFORMATION

Additional Supporting Information may be found online in the supporting information tab for this article.

How to cite this article: Cordeiro IR, Yu R, Tanaka M. Regulation of the limb shape during the development of the Chinese softshell turtles. *Evolution & Development*. 2020;22:451–462. https://doi.org/10.1111/ede.12352